Energy Conversion and Management 264 (2022) 115734

Contents lists available at ScienceDirect

Energy Conversion and Management

journal homepage: www.elsevier.com/locate/enconman

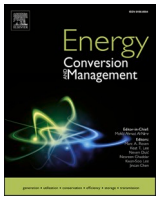

# Process optimization of biomass gasification with a Monte Carlo approach and random forest algorithm

Yi Fang [a], Li Ma [b], Zhiyi Yao [c], Wangliang Li [d], Siming You [a,*]

[a] James Watt School of Engineering, University of Glasgow, Glasgow G12 8QQ, UK
[b] National Key Laboratory of Rotorcraft Aeromechanic, Nanjing University of Aeronautics and Astronautics, Nanjing 210016, China
[c] CBE Eco-Solutions Pte. Ltd., Singapore 117602, Singapore
[d] CAS Key Laboratory of Green Process and Engineering, Institute of Process Engineering, Chinese Academy of Sciences, Beijing 100190, China

ARTICLE INFO

*Keywords:*
Biomass gasification
Kinetic model
Monte Carlo simulation
Machine-learning
Random forest algorithm

ABSTRACT

Gasification technologies have been extensively studied for their potential to convert biomass feedstocks into syngas (a mixture of $CH_4$, $H_2$, and CO mainly) that can be further turned into heat or electricity upon combustion. It is crucial to understand optimal gasification process parameters for practical design and operation for maximizing the potential. This study combined the Monte Carlo simulation approach, gasification kinetic modeling, and the random forest algorithm to predict the optimal gasification process parameters (i.e. water content, particle size, porosity, thermal conductivity, emissivity, shape, and reaction temperature) towards a maximum syngas yield. The Monte Carlo approach randomly generated a data pool of the process parameters following either a normal or uniform distribution, which was then fed into a validated kinetic model to create 2,000 datasets (process parameters and syngas yields). For the random forest model, the mean decrease accuracy and mean decrease Gini were used to assess the importance of the process parameters on syngas yields. The accuracy of the optimization method was evaluated using the coefficient of determination ($R^2$), the root means square error (RMSE), and the mean absolute error (MAE). Generally, the predictions for the normal distribution case were closer to the experimental data obtained from existing literature than that for the uniform distribution case. The model was used to predict the optimal syngas yield and process parameters of wood gasification and it was shown that the predictions were generally in good agreement (<12% difference for the case of normal distribution) with existing experimental results. The method serves as a useful tool for determining optimal gasification process parameters for process and operation design.

## 1. Introduction

The depletion of fossil fuels and greenhouse gas (GHG) emissions are two major issues that have promoted the search for renewable fuels and energy products. Biomass resources are one of the promising sources of renewable energy [1]. It can be converted into electricity, heat, fuels, and chemicals through thermochemical (e.g., gasification and pyrolysis) or biochemical (e.g., anaerobic digestion and fermentation) pathways to relieve the energy and environmental pressures. Among the technologies, gasification has been extensively studied for its potential to recover energy or value-added chemicals from biomass. Specifically, gasification can convert biomass materials into synthesis gas (or syngas) rich in carbon monoxide and hydrogen under an oxygen-deficient condition. Syngas can be further utilized for electricity and/or heat generation or upgraded to produce multifunctional products (e.g., biohydrogen via water–gas shift reactions).

The gasification process involves complex thermochemical reactions which are affected by a variety of process parameters and factors such as biomass types, gasifying agent, particle size, equivalent ratio, reaction temperature, use of catalysts, etc. [2], For example, reducing particle sizes leads to a higher specific surface area, promoting heating and gasification rates and thus $H_2$ yields and carbon conversion efficiencies [3,4]. It was shown that increasing gasification temperature improves the efficiency of the gasification reaction, reducing tar production and effectively contributing to high syngas yield [5,6]. The gasifying agent (i.e. air, steam, oxygen) has been extensively researched and demonstrated that it promotes the decomposition of solid hydrocarbon into lower molecular weight gases (i.e. $CH_4$, $H_2$, and CO) [7]. Use steam as gasification agent significantly promotes the water–gas shift reaction

* Corresponding author.
*E-mail address:* siming.you@glasgow.ac.uk (S. You).

https://doi.org/10.1016/j.enconman.2022.115734
Received 3 March 2022; Received in revised form 21 April 2022; Accepted 7 May 2022
Available online 19 May 2022

**Nomenclature**

| | |
|---|---|
| A | Cross sectional area of the bed ($m^2$) |
| $A_V$ | Specific surface area ($m^2$) |
| cp | Specific heat capacity ($J\,kg^{-1}\,K^{-1}$) |
| D | Diffusivity ($m^2s^{-1}$) |
| d | Diameter (m) |
| F | Mass flow rate ($kg\,s^{-1}$) |
| h | Heat transfer coefficient ($W\,m^{-2}\,K^{-1}$) |
| k | Mass transfer coefficient ($m\,s^{-1}$) |
| M | Molecular weight ($kg\,mol^{-1}$) |
| m | Mass (kg) |
| Nu | Nusselt number (-) |
| q | Heat flux ($W\,m^{-2}$) |
| R | Gas constant (8.314 $J\,mol^{-1}\,K^{-1}$) |
| Re | Reynolds number (-) |
| r | Radius (m) |
| Sc | Schmidt number (-) |
| Sh | Sherwood number (-) |
| T | Temperature (K) |
| t | Time (s) |
| u | Velocity ($m\,s^{-1}$) |
| $L_{bed}$ | Bed height (m) |
| V | Volume ($m^3$) |
| $V_{ad}$ | Volume fraction of ash ($m^3$) |
| $X_B$ | Dry-ash-free biomass conversion rate |
| Y | Mass fraction (-) |

*Greek letters*

| | |
|---|---|
| $\varepsilon$ | Porosity (-) |
| $\rho$ | Density ($kg\,m^{-3}$) |
| $\upsilon$ | Stoichiometric number (-) |
| $\mu$ | Effective viscosity ($kg\,m^{-1}\,s^{-1}$) |
| $\eta$ | Dynamic viscosity ($Pa\,s^{-1}$) |
| $\varepsilon$ | Particle emissivity (-) |
| $\sigma$ | Stefan-Boltzmann constant ($5.67 \times 10^{-8}\,W\,m^{-2}K^{-4}$) |
| $\kappa$ | Thermal conductivity ($W\,m^{-1}\,K^{-1}$) |

*Subscripts*

| | |
|---|---|
| gs | Heat/mass transfer in gas–solid phase |
| g,p | Gas phase in porous biomass particle |
| s,p | Solid phase in porous biomass particle |
| i | Species/component in gas phase with index i |
| j | Species/component in solid phase with index j |
| k | Reaction number with index k |
| p | Particle phase |
| sat | Saturation |
| surf | Surface |
| t | Transient variables |
| vap | Vaporization |
| vol | Volume |
| w | Water |
| P | Particle |
| mfv | Minimum fluidization velocity |

move forward to produce more $H_2$ [8,9]. In contrast, using air as agent produces a higher CO content under the same operation conditions [7]. The effect of catalysts on gasification reaction has been extensively studies, typical catalysts include dolomite catalysts, alkali metal catalysts, and noble metal catalysts. [10]. Fang et al. presented that the noble metal catalysts had excellent properties for biomass gasification in the range of 800–920 K, and it about 98–99% of the carbon in biomass feedstock was converted to syngas [2]. For the gasifier design and process improvement purposes, accurate modelling of biomass conversion during the gasification process is required. Syngas yields are influenced by a number of process parameters (e.g., water content of feedstock, particle porosity, particle shape, and thermal conductivity), which needs to be considered in the modelling analysis.

The composition or type of feedstocks (i.e. wood, crop residues, municipal solid waste (MSW), algae, sludge, etc.) is an important factor affecting biomass gasification. For example, MSW is often a mixture of different waste biomass whose compositions can vary widely across different cities even countries [11]. Meanwhile, wood or waste wood is of relatively consistent compositions and is well suitable for gasification to achieve high syngas yields with e.g., $H_2$ contents of 30–54.5 mmol/$g_{wood}$ and CO contents of 26.8–34.3 mmol/$g_{wood}$ [2]. Wood is also one type of primary biomass and accounts for 53–70 wt% of waste in countries like Egypt, China, Canada, Mexico, Philippines, Greece, and United Kingdom. Accordingly, it has been extensively researched in gasification studies with a pool of data for model validation. Hence, wood is focused by this work as the starting point. It is worth mentioning that the model can always be adapted to suit other types of biomass when relevant data is available for model validation.

Theoretical biomass gasification modeling can be divided into thermodynamic equilibrium and kinetic models. The thermodynamic equilibrium approach applied the method of Gibbs free energy minimization to reveal the thermodynamic boundaries under specific conditions [12–14]. The kinetic approach generally provides a more detailed and accurate description of the gasification process than the equilibrium model. It considers the kinetic information and thermodynamic properties of gasification reactions [15,16].

Stochastic biomass gasification models have been proposed to account for the effects of uncertainties on syngas composition predictions [17,18]. Mazaheri et al. described the gasification process using a stochastic kinetic model based on the Monte Carlo simulation approach. They applied the model to study the influences of process parameters on the efficiency of the conversion process [7]. However, Xing et al. argued that the Monte Carlo simulation-based kinetic models considered a limited number of process parameters and might not be sufficient to demonstrate the complex non-linear relationships in the kinetic parameters (i.e. reaction temperature) and biomass properties (i.e. water content, porosity, density, etc.). They suggested that Machine Learning (ML) algorithms could be used to account for the non-linear relationships for improving the accuracy of gasification modeling.

ML is an artificial intelligence (AI) method widely used in signal processing, function approximation, simulation, and pattern recognition [19]. ML can effectively predict system outputs by learning and mining system features using limited experimental data [20,21]. Among the various ML algorithms, artificial neural networks (ANN) and Random Forest (RF) algorithms are widely used in modeling and optimization. Shahbaz et al. used the ANN model to predict the syngas composition (the model results were in good agreement with experimental results). They found a maximum $H_2$ yield of 79 vol% at 965 K and $CH_4$ yield of 14.93% at 923 K [22]. Xing et al. investigated the influences of gasification parameters (i.e. cellulose fraction, hemicellulose fraction, lignin fraction, and heating rate) on the $H_2$ yield from a fixed bed gasifier using empirical correlations (EC), ANN, and RF algorithms. They compared model predictions with experimental data and found that the ANN and RF models presented high accurate predictions (determination coefficients larger than 0.92), while the EC model showed large deviations in the predictions (determination coefficients$<$0.80). They suggested that the EC model could not characterize complex non-linear relationships accurately. Instead, the ANN and RF models were better suited to

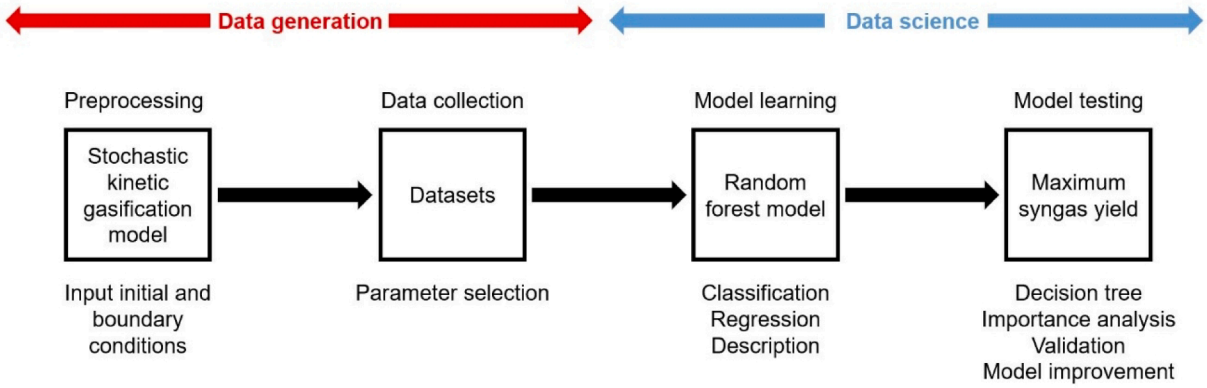


**Fig. 1.** Overview of the methodology.

represent these complex correlations, with the RF model having the highest accuracy [23]. Gopirajan et al. utilized an RF model to optimize the reaction parameters (i.e. biomass characteristics, temperature, pressure, steam/biomass ratio, and reaction time) to improve the energy efficiency, and product quality of gasification. The model achieved an accuracy of 94% and the RF model was more suitable for optimizing the gasification process (e.g., methanation, water gas shift, steam reforming, pyrolysis, and hydrolysis) driven with multiple parameters [21]. However, there are still rare models that could be used to directly predict the optimal gasification process parameters towards maximum syngas yields, while this predicting capability is critical for practical gasification designing and planning.

This study aims to fill the knowledge and capability gaps by developing a stochastic biomass gasification model based on the combination of the MC simulation approach and an RF algorithm. The model is validated against existing experimental data and can predict the maximum syngas yield and associated process parameters (i.e. water content, temperature, particle diameter, porosity, thermal conductivity, emissivity, and particle shape). Additionally, the influences of process parameters towards gasification syngas production are explored based on the developed model.

## 2. Methodology

The research methodology adopted in this study is illustrated in Fig. 1, which consists of 4 stages:

- The kinetic gasification model was developed and validated using experimental data.
- The MC simulation approach (two cases corresponding to uniform and normal distributions, respectively) is combined with the kinetic model to create statistical datasets (process conditions and syngas yields) for RF modeling
- The RF model was trained and tested using 2,000 process parameters and production datasets from uniform and normal distributions, respectively: (water content, particle size, particle porosity, particle shape, thermal conductivity, emissivity, and reaction temperature) and syngas ($H_2$, CO, $CO_2$, $CH_4$, $N_2$) yields.
- Optimal process conditions are predicted and compared with experimental data from literature for model validation and the influences of process parameters on maximum syngas yields are studied.

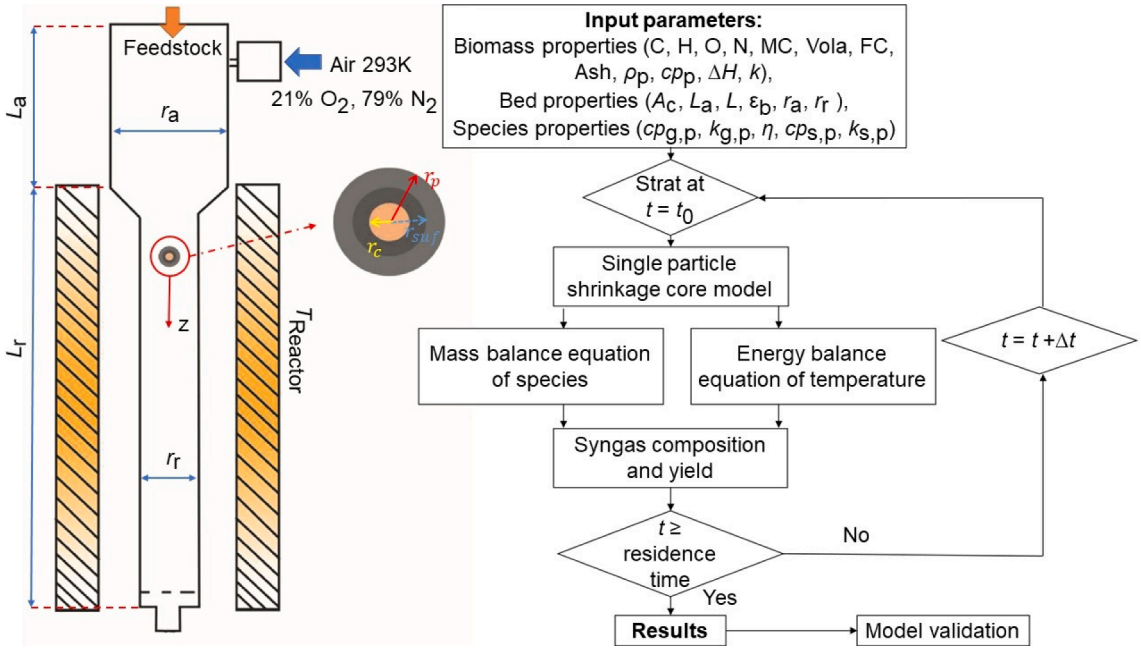


**Fig. 2.** A schematic diagram of the kinetic model coupling the shrinkage core model and fixed bed gasification.

### 2.1. Kinetic model development

#### 2.1.1. Kinetic model description and assumption

In this study, the kinetic model was coupled to a single particle shrinkage core model based on the one-dimensional fixed bed gasification with air being its gasifying agent schemes as shown in Fig. 2. All species are assumed well mixed and moved from top to bottom in the gasifier. The process parameters (i.e. $\rho_{g,\,p,0} = 1.19 kg/m^3$, $Y_{O_2,0} = 0.21, Y_{N_2,0} = 0.79$, $T_{p,0} = 298$ K, and $r = r_0$) were used as the initial and boundary conditions. Biomass particles are porous media, and thus a shrinkage core model was used to achieve reasonable model accuracy. During the thermochemical reactions, the porosity inside a particle increases with time, leading to shrinkage until a certain critical value with the continuous release of syngas or impurities (i.e. particulate matter). It was also considered that homogeneous reactions (e.g., $CO + H_2O \rightarrow CO_2 + H_2$) occurred in the gas phase and heterogeneous reactions (e.g., $C + H_2O \rightarrow CO + H_2$) occurred at the gas and solid phases. The single particle model accounting for biomass particle properties was discretized in the radial direction.

Four solid or liquid species (water, volatiles, fixed carbon, and ash) and six gases ($H_2$, CO, $CO_2$, $CH_4$, $N_2$, and $H_2O$) were considered using a finite volume method and governing equations (mass and energy balance) were used to calculate the gas mixture composition (especially for the yields of $H_2$, CO, and $CH_4$). The following assumptions were established and have been commonly adopted in existing kinetic modeling of fixed bed gasification [24–29].

- Biomass particle was represented in a one-dimensional time domain.
- Solid and gas phases had the same temperature and temperature gradient, the density of the solid phase was the same.
- Gaseous species were ideal gas.
- Gravity was negligible.
- The pressure at the surface of the particles was assumed to be the same as the inside of the reactor.
- The thickness of the reactive zone was constant.

#### 2.1.2. Governing equation

In the kinetic model, the shape and aspect ratio of the shrinking particle do not change, even though the particle size continuously decreases. The considered species include biomass, char, liquid water, syngas, tar, water vapor, and inert gas. Biomass, char, and liquid water are considered by the equations of solid-phase species with their density being modeled, while syngas, tar, water vapor, and inert gas are considered by the equations of gas-phase species with their volume being quantified by the volume of the pores of the particle. In summary, the mass balance of a porous biomass particle is composed of instantaneous particle mass and cumulative mass, and it can be mathematically expressed as [30]:

$$m_{B0} + m_{MC} = \int_{r_c}^{r_p} \rho_p (4\pi r^2) dr + 4\pi r_p^2 \varepsilon_P u \sum_i \rho_{g,p} \tag{1}$$

where $m_{B0}$ is the initial mass of the unreacted particle, $m_{MC}$ is the moisture content of the biomass particle, $\rho_p$ is the density of the biomass particle, $r_p$ is the initial radius of the biomass particle, $r_c$ is the radius of biomass particle upon the finish of the gasification process shown in Fig. 2, u is the velocity of biomass particle in the reactor, $\rho_{g,p}$ is the density of gas phase species.

The mass change of the biomass particle is equal to the cumulative mass of the gas released from the particle. The yield of gas species $Y_{i,g,p}$ is defined by [28]:

$$Y_{i,g,p} = \left\{ \int_0^{\infty} \left[ \int_{r_c}^{r_p} \rho_{g,p} (4\pi r^2) dr + \int_0^t \left( \frac{dm_{g,p}}{dt} \right) dt \right] \cdot E(t) dt \right\} \Big/ (m_{B0} + m_{MC}) \tag{2}$$

where E(t) is defined as the distribution function of residence time for perfectly mixed gas phase species [31]:

$$E(t) = \frac{1}{\tau_s} \bullet \exp\left(\frac{-t}{\tau_s}\right) \tag{3}$$

where the mean gas phase species residence time $\tau_s$ is obtained by dividing the particle mass with the mass flow rate of cumulative mass.

The instantaneous equilibrium equation of continuity (containing mass and energy) is solved by the finite control volume method. The continuity equation in the gas phase accounts for the convective mass transfer and the species produced in the heterogeneous reactions between the solid and gas phases. The mass balance of the overall gas species is expressed as [28]:

$$\begin{aligned} \frac{d(\varepsilon_p \rho_{g,p})}{dt} &= -\frac{1}{r^2}\frac{d}{dr}(r^2 u_{g,p} \varepsilon_p \rho_{g,p}) \\ &+ \frac{1}{r^2}\frac{d}{dr}\left[ r^2 \varepsilon_p D_i \frac{d(\rho_{g,p} Y_{i,g,p})}{dr} \right] + \sum_k \varepsilon_p \dot{r}_{vol,k} \upsilon_{k,i} M_i \\ &+ \sum_k (1-\varepsilon_p) \dot{r}_{suf,k} \upsilon_{k,i} M_i A_v \end{aligned} \tag{4}$$

where $\varepsilon_p$ is porosity of the particle, $\rho_{g,p}$ is density of gas species that can be calculated from the ideal gas law $\rho_{g,p} = \frac{pM}{RT_g}$, $D_i$ is the diffusivity of gas species, $\dot{r}_{vol,k}$ is the volume reaction rate of the reaction numbered with k, $\dot{r}_{suf,k}$ is the surface reaction rate, $\upsilon_{k,i}$ is the stoichiometric number of gas species of the reaction numbered with k, and $M_i$ is the molecular weight of gas species, $A_v$ is the specific surface area, $u_{g,p}$ is the velocity of gas species, as given by:

$$u_{g,p} = \frac{1}{4\varepsilon_p \pi r^2} \int_{r_0}^{r_p} \frac{\left[ \sum_i \varepsilon_p \dot{r}_{vol,k} \upsilon_{k,i} M_i + \sum_i (1-\varepsilon_p) \dot{r}_{suf,k} \upsilon_{k,i} M_i A_v \right] dV}{\rho_{g,p}} dr \tag{5}$$

The composition and yields of the syngas are determined using the source terms of convective mass transfer, diffusive mass transfer, and the species produced in homogeneous and heterogeneous reactions. Each species is assumed to be made of carbon, hydrogen, and oxygen. The mass balance of gas species is expressed as [28]:

$$\begin{aligned} \frac{d(\varepsilon_p \rho_{g,p} Y_{i,g,p})}{dt} &= -\frac{1}{r^2}\frac{d}{dr}(r^2 u_{g,p} \varepsilon_p \rho_{g,p} Y_{i,g,p}) + \frac{1}{r^2}\frac{d}{dr}\left[ r^2 \varepsilon_p D_i \frac{d(\rho_{g,p} Y_{i,g,p})}{dr} \right] \\ &+ \sum_k \varepsilon_p \dot{r}_{vol,k} \upsilon_{k,i} M_i + \sum_k (1-\varepsilon_p) \dot{r}_{suf,k} \upsilon_{k,i} M_i A_v \end{aligned} \tag{6}$$

The mass balance of the solid phase is expressed as [28]:

$$\frac{d}{dt}\left[ \frac{1}{3} \rho_{s,p} (r_p)^3 \right] = \sum_j \dot{r}_{suf,k} \upsilon_{k,j} M_j (r_p)^2 \tag{7}$$

Assuming the gas, liquid, and solid phases of the particle are at the same local temperature, the energy equation is expressed as [28]:

$$\frac{dT_s}{dt} = -\frac{1}{\rho_{s,p} cp_{s,p}} \frac{dq_{s,s}}{dz} + A_v \frac{q_{g,s}}{\rho_{s,p} cp_{s,p}} + \frac{\sum_k \varepsilon_p \dot{r}_{vol,k} \Delta H_k + \sum_k (1-\varepsilon_p) A_v \dot{r}_{suf,k} \Delta H_k}{\varepsilon_p \rho_{g,p} cp_{g,p} + (1-\varepsilon_p) \rho_{s,p} cp_{s,p}} \tag{8}$$

where $q_{s,s} = -\hat{I}^o_p \frac{dT_s}{dz}$ is the conductive heat transfer in the solid phase.$q_{g,s}$ is calculated from the temperature difference (convective and radiative heat transfer) between the solid and gas phases [28]: $q_{g,s} = h_{g,s}(T_g - T_s) + \sigma\varepsilon(T_g^4 - T_s^4)$.

The total energy balance conservation equation about the temperature of the particle combines the gas phase and solid phase, and it is expressed as [28]:

**Table 1**
Gasification reactions.

| Heterogeneous reactions | | | | |
|---|---|---|---|---|
| Reactions | | Kinetic reaction rate (m/s) | $E_a$(kJ/kmol) | Ref. |
| Boudouard | $C + CO_2 \rightarrow 2CO$ | $R_{j,1} = 0.6 \bullet 10^3 T_s \exp(-\frac{26800}{T_s})$ | 222,829 | [32] |
| Water-gas | $C + H_2O \rightarrow CO + H_2$ | $R_{j,2} = 5.7 \bullet T_s \exp(-\frac{15600}{T_s})$ | 129,706 | [33] |
| C partial combustion | $2C + O_2 \rightarrow 2CO$ | $R_{j,3} = 2.3 \bullet T_s \exp(-\frac{11100}{T_s})$ | 79,000 | [34] |
| C complete combustion | $C + O_2 \rightarrow CO_2$ | $R_{j,3}/R_{j,4} = 2.5 \bullet 10^3 \exp(-\frac{6420}{T_g})$ | 27,118 | [35] |
| Methane | $C + 2H_2 \rightarrow CH_4$ | $R_{j,5} = 3.4 \bullet 10^{-3} T_s \exp(-\frac{15600}{T_s})$ | 129,706 | [32] |
| Homogeneous reactions | | | | |
| | Reactions | Kinetic reaction rate (kmol $m^{-3}s^{-1}$) | $E_a$(kJ/kmol) | Ref. |
| CO partial combustion | $CO + \frac{1}{2}O_2 \rightarrow CO_2$ | $R_{i,6} = 1.3 \bullet 10^{11} \varepsilon \exp(-\frac{15105}{T_g}) C_{H_2O}^{0.5} C_{O_2}^{0.5}$ | 125,600 | [27] |
| Water-gas shift | $CO + H_2O \leftrightarrow CO_2 + H_2$ | $R_{i,7} = 2.8\varepsilon \exp\left(-\frac{1511}{T_g}\right)[C_{CO} C_{H_2O} - \frac{\exp\left(-\frac{7914}{T_g}\right) C_{CH_2} C_{H_2}}{0.0265}]$ | 12,560 | [36] |
| Steam-methane reforming | $CH_4 + H_2O \leftrightarrow CO + 3H_2$ | $R_{i,8} = 3.0 \bullet 10^8 \varepsilon \exp(-\frac{15083}{T_g}) C_{CH_4} C_{H_2O}$ | 30,000 | [36] |
| $H_2$ combustion | $H_2 + \frac{1}{2}O_2 \rightarrow H_2O$ | $R_{i,9} = 3.5 \bullet 10^8 \varepsilon \exp(-\frac{3670}{T_g}) C_{H_2}^{1.1} C_{O_2}^{1.1}$ | 30,514 | [37] |

**Table 2**
List of model inputs and parameters [27,28,38].

| | | |
|---|---|---|
| Characteristics of gasifier reactor | $L$ (m) | 0.50 |
| | $L_a$(m) | 0.25 |
| | $A_c$($m^2$) | 0.07 |
| | $\varepsilon_b$(-) | 0.40 |
| | Biomass resident time (sec) | 360.00 |
| Species properties | $cp_{g,p}$(J $kg^{-1}$ $K^{-1}$) | $1053.92\text{-}0.40T_g + 9.55 \times 10^{-4}T_g^2\text{-}5.73 \times 10^{-7}T_g^3 + 6.99 \times 10^{-11}T_g^4$ |
| | $cp_{s,p}$(J $kg^{-1}$ $K^{-1}$) | 1350.00 |
| | $k_{g,p}$(W $m^{-1}$ $K^{-1}$) | $3.14 \times 10^{-4}T_g^{0.78}/(1\text{-}\frac{0.71}{T_g} + \frac{2121.70}{T_g^2})$ |
| | $k_{s,p}$(W $m^{-1}$ $K^{-1}$) | 0.08 |
| | $\hat{I}\cdot(10^{-5}$Pa $s^{-1})$ | $\text{-}1.22 \times 10^{-3} + 0.01T_g\text{-}7.45 \times 10^{-4}T_g^2\text{-}5.73 \times 10^{-7}T_g^3 + 6.99 \times 10^{-11}T_g^4$ |
| Time step | $\Delta t$(sec) | $10^{-3}$ |
| Finite volume length | $\Delta z$(m) | 0.01 |
| Equivalent ratio | (-) | 0.29 |
| Feeding rate | (kg/h) | 10 |

$$\frac{d(\varepsilon_p \rho_p cp_p T_p)}{dt} = -\frac{1}{r^2}\frac{d}{dr}(r^2 \varepsilon_p \rho_{g,p} cp_{g,p} u_{g,p} T_p) + \frac{1}{r^2}\frac{d}{dr}[r^2(1\text{-}\varepsilon_p)\hat{I}^o_p \frac{dT_p}{dr}] + \sum_i \frac{1}{r^2}\frac{d}{dr}[r^2 \varepsilon_p cp_{g,p} D_i T_p \frac{d(\rho_{g,p} Y_{i,g,p})}{dr}] + \sum_k \varepsilon_p \dot{r}_{vol,k} \Delta H_k + \sum_k (1\text{-}\varepsilon_p) A_v \dot{r}_{suf,k} \Delta H_k \quad (9)$$

All reaction rate constants are expressed in the first-order Arrhenius form, and the kinetic parameters and heat of reactions are summarized in Table 1. In addition, the kinetic rate expressions of 9 gasification reactions included in the model are listed in Table 1. The kinetic rate of methanation is much lower than that of the other heterogeneous reactions. $CH_4$ is produced rapidly at the high partial pressure of $H_2$ in reaction (8). The catalytic effects of metal components (e.g., Ca, Na, and K) on gasification reactions are not considered in this model and are worth future exploration as many studies have shown that they have a significant influence on biomass gasification reactions for high ash content biomass [2].

### 2.1.3. Numerical solution procedure

A schematic diagram of the kinetic model is shown in Fig. 2. The governing equations are discretised using a finite volume scheme, and a representative particle was chosen and modelled as a shrinkimg sphere. The particle moves toward the z-direction to the bottom of the reactor with a velocity of *u*. Input parameters include biomass properties (ΔH is the enthalpy of biomass, and *k* is the heat conductivity of biomass

**Table 3**
Summary of process parameters for constructing the probability distributions.

| Experiments/ process parameters | Feedstock | Water content (wt.%) | Porosity | Size (mm) | Thermal conductivity (W/mK) | Emissivity | Shape | Temperature (K) |
|---|---|---|---|---|---|---|---|---|
| [27] | Wood | 8.00 | 0.28 | 2.00 | 0.20 | 0.75 | sphere | 1,073.00 |
| [40] | Wood | 10.00 | – | 0.50–5.00 | 0.04–0.18 | – | – | 673.00–1,673.00 |
| [41] | Wood | 15.00 | 0.28–0.44 | 0.30–3.00 | – | – | – | 1,123.00–1,198.00 |
| [42] | Wood | 11.70 | – | 0.15–0.25 | 0.12 | – | flat | 973.00–1,173.00 |
| [43] | Wood | 12.00 | – | 2.00 | – | 0.86–0.90 | flat | 1,053.00–1,113.00 |
| [44] | Wood | 4.40–15.18 | 0.48 | 25.40 | – | – | cylinder | 1,073.00–1,173.00 |
| [45] | Wood | 9.04 | – | 0.3–1.00 | – | – | sphere | 1,073.00–1,273.00 |
| [46] | Wood | 7.00–16.10 | – | 6.00 | – | – | cylinder | 1,073.00–1,273.00 |
| [47] | Wood | 11.45 | – | 1.00–10.00 | | | flat | 1,173.00–1,323.00 |
| [48] | Wood | 9.50 | 0.52 | 1.95 | – | 0.85 | cylinder | 1,073.00–1,273.00 |

**Table 4**
Means and standard deviations for the distributions of the process parameters.

| Input factors | Range | $\mu$ | $\sigma$ |
|---|---|---|---|
| Feedstock | | | |
| Water content (wt.%) | 9.29–11.29 | 10.28 | 0.36 |
| Porosity | 0.20–0.35 | 0.26 | 0.03 |
| Size (mm) | 1.00–2.00 | 1.50 | 0.19 |
| Thermal conductivity (W/mK) | 0.18–0.22 | 0.20 | $0.71 \times 10^{-2}$ |
| Emissivity | 0.72–0.77 | 0.75 | $0.89 \times 10^{-2}$ |
| Shape | – | – | – |
| Reactor | | | |
| Temperature (K) | 973.00 – 1,173.00 | 1,075.99 | 34.95 |

particle), gasifier bed properties ($L$ is the length of gasifier reactor, $L_a$ is the length of the region above gasifier reactor, $A_c$ is the cross sectional area of gasifier reactor, and $\varepsilon_b$ is the porosity of fixed bed), and species properties ($cp_{g,p}$ and $cp_{s,p}$ are specific heat capacity of gas-phase and solid-phase species, $k_{g,p}$ and $k_{s,p}$ are heat conductivity of gas-phase and solid-phase species, and Î· is dynamic viscosity). The values of model input and parameters are shown in Table 2.

### 2.2. Monte Carlo simulation

The MC simulation is a probabilistic approach based on a randomization process that involves probability distributions of data variables collected based on past data, and theoretical probability distribution [39]. For an actual gasification process, numerous particles are involved and there are variations in the process parameters. To account for the variations and potential uncertainty of the parameters, a stochastic kinetic model was generated by combing the above kinetic model with the MC approach. It is unclear which probability distribution is most suitable for describing the process parameters for MC simulation. Hence, in this work, two types of probability distributions (i.e. uniform and normal) were explored and defined based on experimental data to generate stochastic values for major process parameters (i.e. water content, particle size, porosity, thermal conductivity, emissivity, shape, and reaction temperature) for the MC simulation. The MC approach for this model was to take random values for process parameters in uniform and normal distributions, and the data based on which the distributions were defined are from 10 experimental studies on fixed bed gasifier (wood as the feedstock) as summarized in Table 3. The water content ranges from 9.29 to 11.29 wt%, the porosity data ranges from 0.20 to 0.35, the size data ranges from 1.00 to 2.00 mm, the thermal conductivity data ranges from 0.18 to 0.22 W/mK, the emissivity data ranges from 0.72 to 0.77, the particle shape data is spherical, cylinder and flat, and the reaction temperature data ranges from 973.00 to 1,173.00 K.

The mean ($\mu$) and standard deviation ($\sigma$) of the distributions (uniform and normal) for each process parameter were calculated by Eq. (10) & (11) and were listed in Table 4.

$$\mu = \frac{\sum_{a=1}^{N}(x_a)}{N} \tag{10}$$

$$\sigma = \sqrt{\frac{1}{N}\sum_{a=1}^{N}(x_a-\mu)^2} \tag{11}$$

where $N$ is the number of parameters, and $x_i$ is the individual value of a parameter.

### 2.3. Random forest model evaluation

#### 2.3.1. Evaluation metrics for decision tree

The RF algorithm is an ensemble learning method based on bagging [49]. The standard binary decision tree used to solve this regression problem is defined with several branches, a root, several nodes, and leaves. Basically, a branch is a chain of nodes from the root to the leaves, with each node referring to an attribute [50]. The splitting criteria for the regression tree is also known as Classification and Regression Trees (CART). During the growth of each regression tree, a Gini Index (GI) is the best principle to judge the classification quality in the CART [51]. The dataset D(o) is classified into subset D(s) (containing the elements of all process parameters) and the GI for each subset was expressed as Eq.

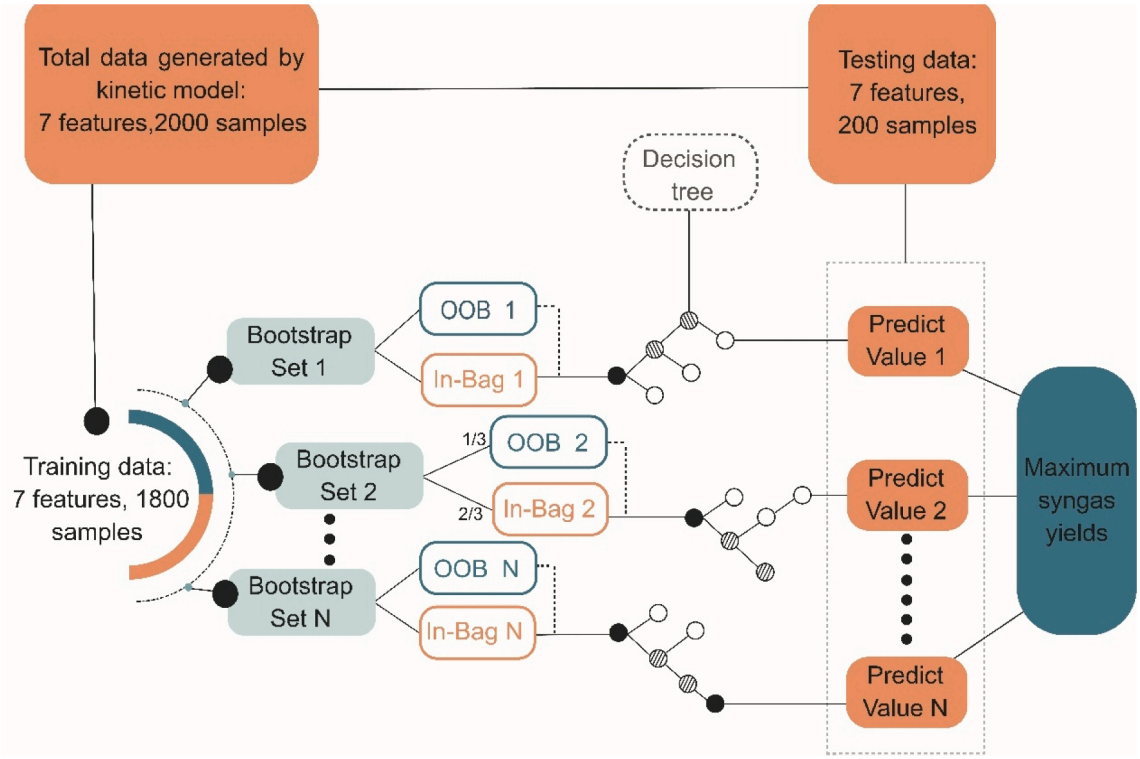


**Fig. 3.** The schematic diagram of the topological structure of the RF algorithm.

**Table 5**
Composition of feedstocks and gasifier process parameters from three existing experimental studies.

| | Garcia-Bacaicoa et al. [56] | Jayah et al. [57] | Zainal et al. [58] |
|---|---|---|---|
| **Feedstock** | Wood | Wood | Wood |
| C (wt.%) | 35.12 | 50.60 | 46.40 |
| H (wt.%) | 7.57 | 6.50 | 5.70 |
| O (wt.%) | 56.96 | 42.00 | 47.70 |
| N (wt.%) | – | 0.20 | 0.20 |
| Ash (wt.%) | 0.32 | 0.70 | 1.10 |
| Volatile matter (wt. %) | 60.76 | 80.10 | – |
| Fix carbon (wt.%) | 9.92 | 19.20 | – |
| Water content (wt. %) | 29.00 | 14.50 | – |
| Mean particle size (mm) | 40.00 | 44.00 | 50.00 |
| Mean air flowrate (kg/h) | 36.70 | 34.60 | – |
| Reaction temperature (K) | 1,365.00 | 1,273.00 | 1,273.00 |
| Gasifier type | Fixed | Fixed | Fixed |

(12). The GI value reflects the purity of the subset. The lower GI value implies the higher quality of classification based on the optimal attribute $k^*$. Finally, the minimum GI value based on the $k^*$ is selected as the result, and it expressed as Eq.13.

$$\text{Gini\_index}(D(o),\ k^*) = \sum \frac{|D(s)|}{|D(o)|}\ \text{Gini}(D(s)) \tag{12}$$

$$k^* = \text{argmin}\text{Gini\_index}(D(o), k^*) \tag{13}$$

The schematic topological architecture of the RF approach is shown in Fig. 3. The regression tree is trained by a bootstrap technique that randomly selects 2/3 of the training data as In Bag (IB) data, and the unselected training data were called Out Of Bag (OOB) data. The OOB data not involved in the training of the regression tree can be used to determine the optimal number of trees by a trial-and-error method [52]. The ultimate predictions of the trained RF model are the average predictions of all trees. The number of trees is chosen to be sufficiently large so that a stabilized OOB error can be achieved. In this study, the number of trees tested is from 1 to 500, and the number of process parameters set at each split is 6. The modelling process ends when the OOB data error has stabilized (being constant). This improves the usage of computational resources). The model was run using a PC with Intel Core i9 10900 K 5.3 GHz processor and 64 GB of RAM, running Windows 10. The splitting criterion for each decision tree depends on the importance of the process parameters which is determined by the value of the percentage increase in mean squared error (%IncMSE) and the total decrease in node impurity (IncNodePurity). The value of %IncMSE is the normalisation of the average of the difference across all trees by the standard deviation: $\Delta MSE/MSE_0 \times 100\%$ [53]. The value of IncNodePurity is measured by Gini index, which averages the sum of overall number of trees when the variables are split at each node [54].

### 2.3.2. Evaluation metrics for model performance

The root mean square error (RMSE), the metric determination coefficient ($R^2$), and the mean absolute error (MAE) are common metrics to measure the accuracy of a RF model in regression analysis by comparing the error between the predicted data and the test data [55]. Lower values for RMSE and MAE will imply the model is more accurate while higher values for $R^2$ will imply the model is more accurate. RMSE measures the standard deviation of residuals and is expressed in Eq.15. $R^2$ represents the proportion of the variance in the dependent process parameter and is calculated by Eq.16. MAE measures the average of the residuals in the dataset, which is expressed in Eq.17.

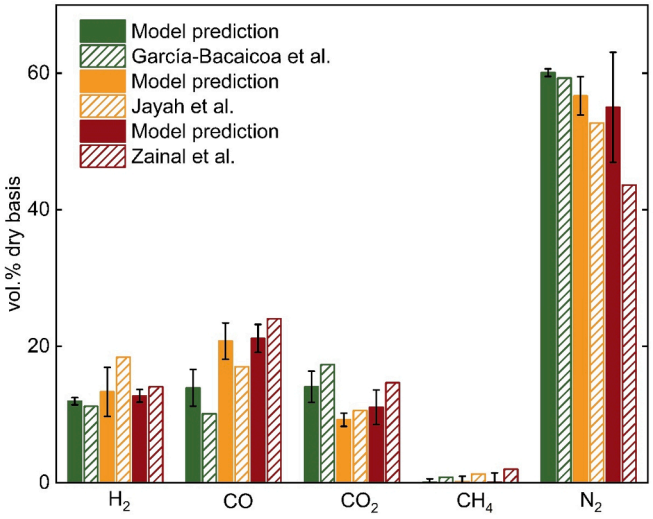


**Fig. 4.** Comparisons between the kinetic module predictions and experimental results.

$$\text{RMSE} = \sqrt{\frac{1}{N}\sum (y_{predict}\text{-}y_{test})^2} \tag{15}$$

$$R^2 = 1\text{-}\frac{\sum (y_{predict}\text{-}y_{test})^2}{\sum (y_{predict}\text{-}\bar{y})^2} \tag{16}$$

$$\text{MAE} = \frac{1}{N}\sum |y_{predict}\text{-}y_{test}| \tag{17}$$

where $N$ is the total number of total data, $y_{predict}$ is the value of prediction, $y_{test}$ is the value of a testing data, $\bar{y}$ is the mean value of all the data. The validation of the RF model was conducted by comparing its predictions with experimental data gathered from the literature.

## 3. Results and discussion

### 3.1. Kinetic model validation

The experimental process parameters (Table 5) of Garcia-Bacaicoa et al. [56], Jayah et al. [57], and Zainal et al. [58] were inputted into the kinetic model to predict the syngas ($H_2$, CO, $CO_2$, $CH_4$, and $N_2$) yields for validation. Fig. 4 shows the comparison between the prediction of syngas yields and the experimental results. The predicted yields of syngas are within 6.6% of the experimental results of Garcia-Bacaicoa et al. [44]. The difference between the experimental and modeling results could be attributed to the fact that only the composition of wood was applied as input parameters while 10–17% polyethylene was mixed with wood as the feedstock for the experiments. This is one of the limitations of the current model based on the consideration of biomass gasification, which warrants further improvement. The predicted yields of syngas are within 12.8% of the experimental results of Jayah et al. [45]. A comparison of $H_2$/CO ratio shows that the error is 2.25% against the experimental data of Garcia-Bacaicoa et al. [44], 5.75% of Jayah et al. [45], and 2.98% of Zainal et al. [46].

### 3.2. Random forest model

The stochastic kinetic model was used to generate 2,000 datasets based on the uniform and normal distributions, respectively. The RF model was used to determine the importance of process parameters on the syngas yields and to find the optimal process parameters leading to the maximum syngas yield.

**Table 6**
Quality indicators of RF modeling based on the training data (uniform and normal distributions).

| | Uniform distribution | | | Normal distribution | | |
|---|---|---|---|---|---|---|
| | **RMSE** | **$R^2$** | **MAE** | **RMSE** | **$R^2$** | **MAE** |
| $CH_4$ | 2.516 $\times 10^{-8}$ | 0.996 | 2.556 $\times 10^{-5}$ | 3.526 $\times 10^{-19}$ | 0.994 | 1.511 $\times 10^{-10}$ |
| $H_2$ | 2.468 $\times 10^{-8}$ | 0.994 | 2.009 $\times 10^{-5}$ | 3.555 $\times 10^{-19}$ | 0.994 | 1.265 $\times 10^{-10}$ |
| CO | 9.114 $\times 10^{-6}$ | 0.998 | 4.686 $\times 10^{-4}$ | 1.177 $\times 10^{-16}$ | 0.997 | 2.827 $\times 10^{-9}$ |

### 3.2.1. Decision tree

The results of the quality evaluation of the RF model for the uniform and normal distribution cases are shown in Table 6. For the uniform distribution case, the value of RMSE, $R^2$, and MAE is 2.516 × 10-8, 0.996, and 2.556 × 10-5 for $CH_4$; 2.468 × 10-8, 0.994, and 2.009 × 10-5 for $H_2$; 9.114 × 10-6, 0.998, and 4.686 × 10-4 for CO. RMSE decreased sharply and remained stable as the number of trees increases. $R^2$ increased gradually and remained stable. The best numbers of the decision tree ($N_{tree\text{-}best}$) for $CH_4$, $H_2$, and CO are 292, 283, and 239 as shown in Fig. 5 (a). For the normal distribution, the values of RMSE, $R^2$, and MAE are 3.526 × 10-19, 0.994, and 1.511 × 10-10 for $CH_4$; 3.555 × 10-19, 0.994, and 1.265 × 10-10 for $H_2$; 1.177 × 10-16, 0.997, and 2.827 × 10-9 for CO. For $CH_4$, $H_2$, and CO, the best numbers of the decision tree ($N_{tree\text{-}best}$) are 143, 233, and 247 as shown in Fig. 5 (b).

### 3.2.2. Variable importance

Fig. 6 (a) and (b) show the importance of process parameters on the syngas yield based on the values of %IncMSE and IncNodePurity. High values of these two metrics indicate high importance of a parameter on syngas yields. The values of %IncMSE (17.04–20.30% for uniform distribution and 14.97–17.76% for normal distribution) and IncNodePurity (0.008–0.009 for uniform distribution and 0.024–0.038 for normal distribution) for temperature are higher than the other process parameters in both the uniform and normal distribution cases, so temperature has the greatest impact on syngas yields. Furthermore, it is also shown that the yields of $H_2$ and CO are strongly influenced by temperature.

The values of %IncMSE and IncNodePurity for the particle size for the uniform distribution case are 21.51–25.61% and 0.014–0.021, and 7.30–8.91% and 0.028–0.053 for the normal distribution case. These indicate that, following temperature, particle size has a relatively high impact on the syngas yield compared to the other process parameters (particle shape (%IncMSE = 8.13–17.04%, IncNodePurity = 0.003–0.004 for uniform distribution, and %IncMSE = 1.48–3.25%, IncNodePurity = 0.006–0.008 for normal distribution)).

The values of %IncMSE and IncNodePurity indicated that water content has a minor impact on syngas yield (the value of %IncMSE and IncNodePurity for the uniform distribution case is 3.60–10.15% and 0.001–0.003, and 7.30–9.91% and 0.021–0.081 for the normal distribution case). Both the values of %IncMSE and IncNodePurity in the uniform distribution and the normal distribution cases indicated that the emissivity, the thermal conductivity, and the particle porosity on syngas yield can be neglected.

### 3.2.3. Quality evaluation of RF modeling against the testing data

The validation of the quality of the RF model was achieved by comparing the predictions with the testing data as shown in Table 7 and Fig. 7. For the uniform distribution case, the values of RMSE, $R^2$, and MAE are 1.779 × 10-4, 0.996, and 6.950 × 10-5 for $CH_4$; 1.491 × 10-4, 0.994, and 5.258 × 10-5 for $H_2$; 2.805 × 10-3, 0.996, and 1.206 × 10-3 for CO. For the normal distribution case, the values of RMSE, $R^2$, and MAE are 7.242 × 10-10, 0.962, and 4.230 × 10-10 for $CH_4$; 4.700 × 10-10, 0.967, and 3.041 × 10-10 for $H_2$; 1.102 × 10-8, 0.982, and 7.397 × 10-9 for CO. The Fig. 7 shows the predictions of the RF model for both the uniform and normal distribution cases agree with the testing data.

### 3.2.4. Process optimization

The water content, particle size, and reaction temperature were

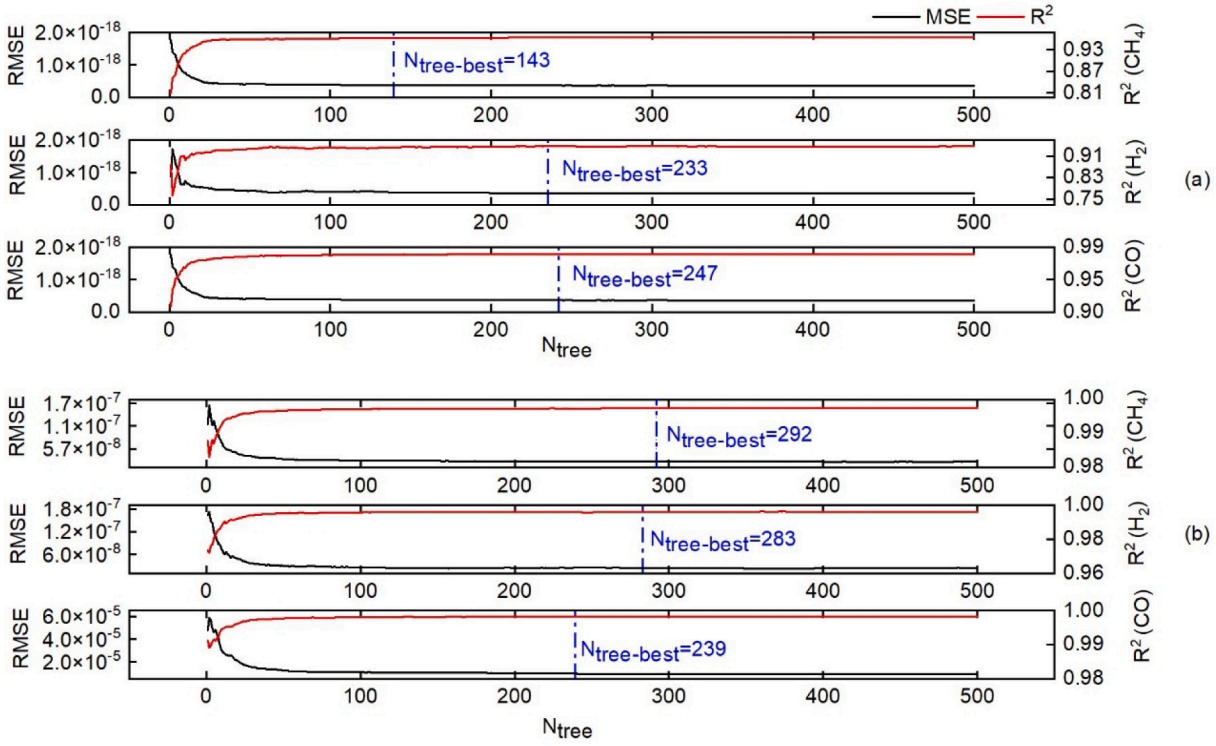


**Fig. 5.** Test results for determining the optimal tree numbers in RF modeling for $CH_4$, $H_2$, and CO ((a) uniform and (b) normal distributions).

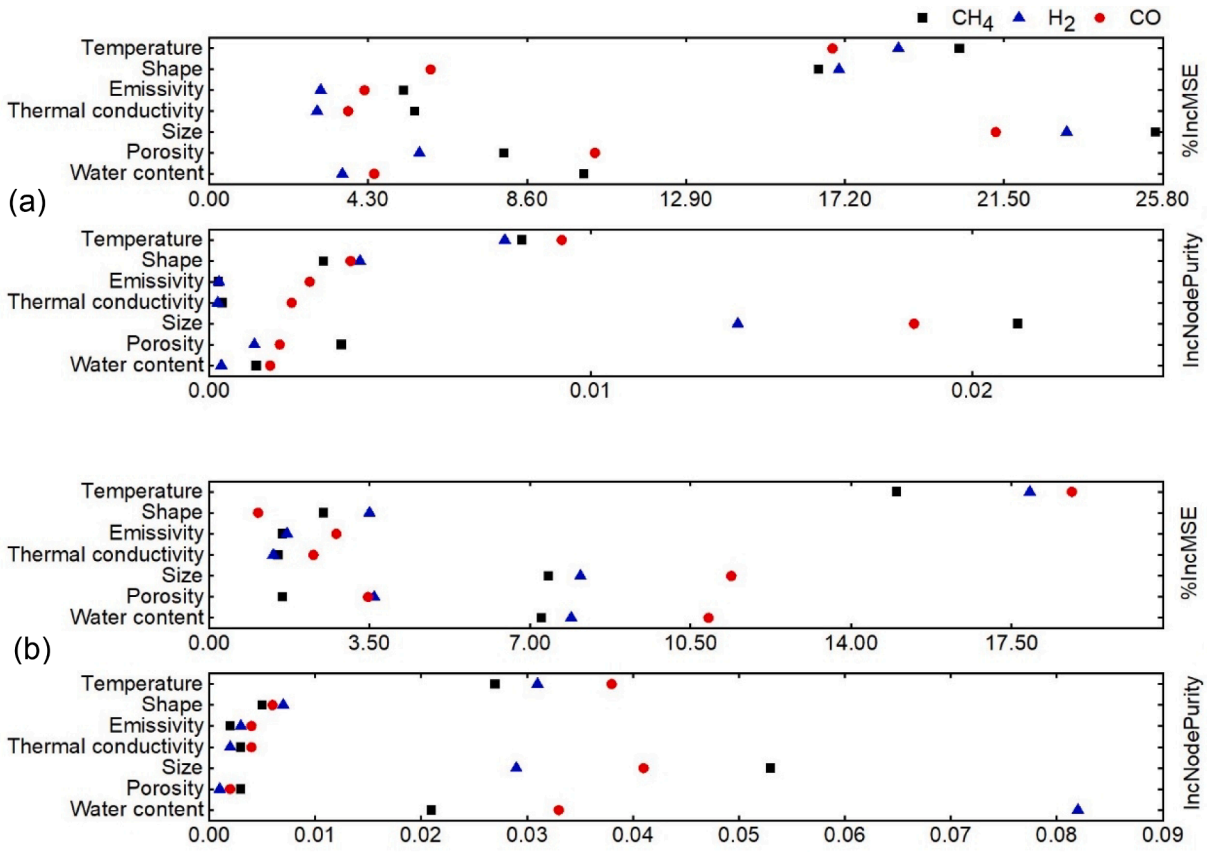


**Fig. 6.** Measured relative importance of each input parameter for syngas yield ((a) uniform and (b) normal distributions).

**Table 7**
Quality indicators of the RF modeling based on the testing data (uniform and normal distributions).

| | Uniform distribution | | | Normal distribution | | |
|---|---|---|---|---|---|---|
| | RMSE | $R^2$ | MAE | RMSE | $R^2$ | MAE |
| $CH_4$ | 1.779 $\times 10^{-4}$ | 0.996 | 6.950 $\times 10^{-5}$ | 7.242 $\times 10^{-10}$ | 0.962 | 4.230 $\times 10^{-10}$ |
| $H_2$ | 1.491 $\times 10^{-4}$ | 0.994 | 5.258 $\times 10^{-5}$ | 4.700 $\times 10^{-10}$ | 0.967 | 3.041 $\times 10^{-10}$ |
| CO | 2.805 $\times 10^{-3}$ | 0.996 | 1.206 $\times 10^{-3}$ | 1.102 $\times 10^{-8}$ | 0.982 | 7.397 $\times 10^{-9}$ |

considered to have a higher impact on the syngas yields as compared to other process parameters as shown above. The RF model predicts the maximum yields of $CH_4$, $H_2$, and CO as 0.19 × 10-2, 2.43 × 10-2, and 40.78 × 10-2mol/$kg_{feedstock}$ for the uniform distribution case and 0.17 × 10-2, 2.31 × 10-2, and 37.89 × 10-2 mol/$kg_{feedstock}$ for the normal distribution case are shown in Table 7. It is also shown that the predicted optimal parameters for the normal distribution case are closer to the experimental data than the uniform distribution case. The results indicated that the normal distribution is a more reasonable representation of the actual process parameters.

## 4. Conclusion

In this study, a stochastic biomass gasification model based on the combination of the MC simulation approach and an RF algorithm is developed. The model was used to optimize the fixed bed air gasification with wood as feedstock for a broad range of process parameters. The parameters importance analysis of the RF model showed that particle size, reaction temperature, and water content have a high influence on the syngas yield. However, the effects of particle shape, emissivity, thermal conductivity, and porosity on syngas yield can be negligible during the gasification process. The predictions of syngas yield in the normal distribution case are more informative and reliable, which fits the experimental better than the uniform one. The predictions for the normal distribution case were closer to the experimental data obtained from existing literature than that for the uniform distribution case. The model was used to predict the optimal syngas yield and process parameters of wood gasification and it was shown that the predictions were generally in good agreement (<12% difference for the case of normal distribution) with existing experimental results as shown in Table 8. The model developed in this work could be used for determining the optimal process parameters for the techno-economic analysis and life cycle assessment towards better system and process designs.

It is worth noting that some factors have not been included in this study partially due to lack of relevant data. For example, ER is not directly considered by the model. However, this factor is closely related to the reaction temperature and particle size both of which are modelled, and thus is implicitly considered by the developed model. Therefore, a fixed ER = 0.29 (obtained from the literature) was applied in this study. In addition, tar formation is considered as an intermediate factor of the kinetic model affecting the syngas yield. As this study focuses on syngas yield, tar production is not analyzed as the outputs of the model. The developed the framework could be further adapted to include the additional parameters when associated data is available in the future.

*CRediT authorship contribution statement*

**Yi Fang:** Conceptualization, Data curation, Formal analysis, Investigation, Methodology, Validation, Writing – original draft. **Li Ma:** Writing – review & editing. **Zhiyi Yao:** Writing – review & editing.

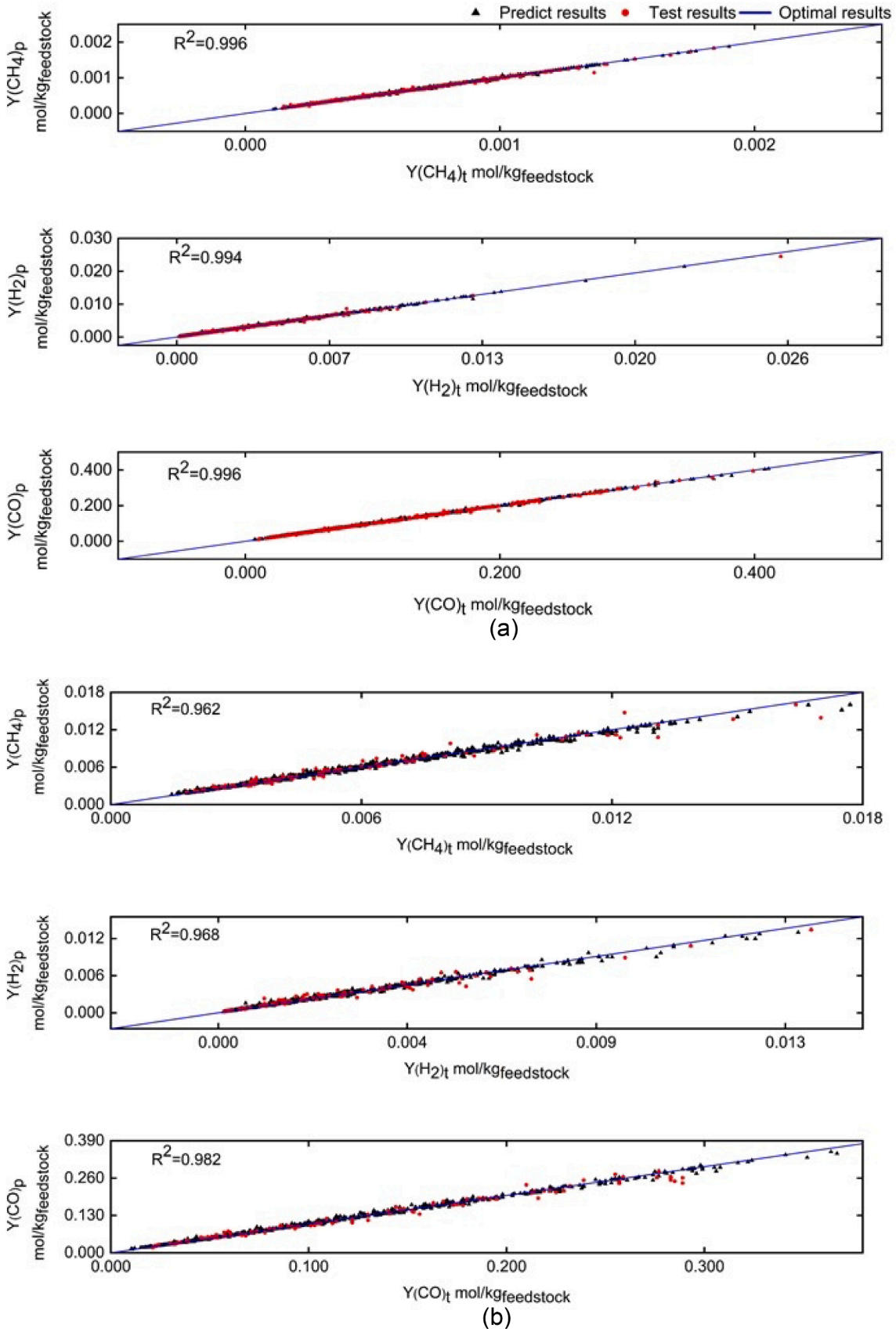


**Fig. 7.** Validation results of RF model for syngas yield ((a) uniform and (b) normal distributions).

**Table 8**
Comparison of the syngas yield and optimal process parameters from the RF model to the experimental data.

| | | $CH_4$ | | | | $H_2$ | | | | CO | | | |
|---|---|---|---|---|---|---|---|---|---|---|---|---|---|
| | | Prediction | | Experiment | | Prediction | | Experiment | | Prediction | | Experiment | |
| | | Uniform[#] | Normal | [46] | [59] | Uniform | Normal | [60] | [61] | Uniform | Normal | [62] | [63] |
| Maximum yield ($mol/kg_{feedstock}$) | | $0.19 \times 10^{-2}$ | $0.17 \times 10^{-2}$ | $0.17 \times 10^{-2}$ | $0.17 \times 10^{-2}$ | $2.43 \times 10^{-2}$ | $2.31 \times 10^{-2}$ | $2.23 \times 10^{-2}$ | $2.30 \times 10^{-2}$ | $40.78 \times 10^{-2}$ | $37.89 \times 10^{-2}$ | $38.23 \times 10^{-2}$ | $33.83 \times 10^{-2}$ |
| Process conditions | Water content (wt.%) | 11.20 | 10.86 | 8.35 | 7.40 | 10.80 | 10.80 | 8.22 | 8.00 | 11.10 | 11.10 | 9.71 | 12.00 |
| | Size (mm) | 2.00 | 1.90 | 2.50 | 2.00 | 1.96 | 1.96 | 1.20 | – | 2.00 | 1.99 | 1.00 | 7.00 |
| | Temperature (K) | 1,005.56 | 995.79 | 1,013.00 | 1,073.00 | 1,172.10 | 1,172.10 | 1,173.00 | 1,173.00 | 1,148.27 | 1,148.27 | 1,140.00 | 1,123.00 |

[#] Parameter distribution applied.

**Wangliang Li:** Funding acquisition, Writing – review & editing. **Siming You:** Supervision, Writing – review & editing, Conceptualization, Funding acquisition, Investigation, Project administration, Validation, Writing – review & editing.

## Declaration of Competing Interest

The authors declare that they have no known competing financial interests or personal relationships that could have appeared to influence the work reported in this paper.

## Acknowledgement

Siming You would like to acknowledge the financial support from the UK Engineering and Physical Sciences Research Council (EPSRC) Programme Grant (EP/V030515/1), Supergen Bioenergy Hub Rapid Response Funding (RR 2022_10), and Royal Society Research Grant (RGS\R1\211358). Wangliang Li would like to thank the financial support from the National Natural Science Foundation of China (No. 21878313). The authors would like to thank Ms. Yang Fang for supporting the design of Figs. 2 and 3. All data supporting this study are provided in full in the 'Methodology' and 'Results and Discussion' sections of this paper.

## References

[1] Fang Y, Li Y, Ahmed A, You S. Development, economics and global warming potential of lignocellulose biorefinery. Biomass: Biofuels, Biochemicals; 2021. p. 1–13.
[2] Fang Y, Paul MC, Varjani S, Li X, Park Y-K, You S. Concentrated solar thermochemical gasification of biomass: Principles, applications, and development. Renew Sustain Energy Rev 2021;150:111484.
[3] Lv P, Xiong Z, Chang J, Wu C, Chen Y, Zhu J. An experimental study on biomass air–steam gasification in a fluidized bed. Bioresour Technol 2004;95:95–101.
[4] Luo S, Xiao B, Hu Z, Liu S, Guo X, He M. Hydrogen-rich gas from catalytic steam gasification of biomass in a fixed bed reactor: Influence of temperature and steam on gasification performance. Int J Hydrogen Energy 2009;34:2191–4.
[5] De Lasa H, Salaices E, Mazumder J, Lucky R. Catalytic steam gasification of biomass: catalysts, thermodynamics and kinetics. Chem Rev 2011;111:5404–33.
[6] Li X, Grace J, Lim C, Watkinson A, Chen H, Kim J. Biomass gasification in a circulating fluidized bed. Biomass Bioenergy 2004;26:171–93.
[7] Mazaheri N, Akbarzadeh A, Madadian E, Lefsrud M. Systematic review of research guidelines for numerical simulation of biomass gasification for bioenergy production. Energy Convers Manage 2019;183:671–88.
[8] Kalinci Y, Hepbasli A, Dincer I. Biomass-based hydrogen production: a review and analysis. Int J Hydrogen Energy 2009;34:8799–817.
[9] Inayat A, Ahmad MM, Mutalib MA, Yusup S. Effect of process parameters on hydrogen production and efficiency in biomass gasification using modelling approach. Journal of Applied Sciences(Faisalabad) 2010;10:3183–90.
[10] Wei L, Xu S, Zhang L, Liu C, Zhu H, Liu S. Steam gasification of biomass for hydrogen-rich gas in a free-fall reactor. Int J Hydrogen Energy 2007;32:24–31.
[11] Kambo HS, Dutta A. A comparative review of biochar and hydrochar in terms of production, physico-chemical properties and applications. Renew Sustain Energy Rev 2015;45:359–78.
[12] Puig-Arnavat M, Bruno JC, Coronas A. Modified thermodynamic equilibrium model for biomass gasification: a study of the influence of operating conditions. Energy Fuels 2012;26:1385–94.
[13] Srinivas T, Gupta A, Reddy B. Thermodynamic equilibrium model and exergy analysis of a biomass gasifier. J Energy Res Technol 2009;131.
[14] Formica M, Frigo S, Gabbrielli R. Development of a new steady state zero-dimensional simulation model for woody biomass gasification in a full scale plant. Energy Convers Manage 2016;120:358–69.
[15] Z. Wei, C. Khor, W. Rahim, N. Razak, M. Ishak, M. Rosli, et al. **Mechanical aspects analysis of the cyclone gasifier design via finite element method.** AIP Conference Proceedings. AIP Publishing LLC2018. Article 020047.
[16] Baggio P, Baratieri M, Fiori L, Grigiante M, Avi D, Tosi P. Experimental and modeling analysis of a batch gasification/pyrolysis reactor. Energy Convers Manage 2009;50:1426–35.
[17] Guo B, Li D, Cheng C, Lü Z-A, Shen Y. Simulation of biomass gasification with a hybrid neural network model. Bioresour Technol 2001;76:77–83.
[18] Weber K, Li T, Løvås T, Perlman C, Seidel L, Mauß F. Stochastic reactor modeling of biomass pyrolysis and gasification. J Anal Appl Pyrol 2017;124:592–601.
[19] İskenderoğlu FC, Baltacioğlu MK, Demir MH, Baldinelli A, Barelli L, Bidini G. Comparison of support vector regression and random forest algorithms for estimating the SOFC output voltage by considering hydrogen flow rates. Int J Hydrogen Energy 2020;45:35023–38.

[20] Ceylan Z, Ceylan S. Application of machine learning algorithms to predict the performance of coal gasification process. In: Applications of Artificial Intelligence in Process Systems Engineering; Elsevier 2021.. p. 165–86.
[21] Gopirajan PV, Gopinath KP, Sivaranjani G, Arun J. Optimization of hydrothermal gasification process through machine learning approach: Experimental conditions, product yield and pollution. J Cleaner Prod 2021;306:127302.
[22] Shahbaz M, Taqvi SA, Loy ACM, Inayat A, Uddin F, Bokhari A, et al. Artificial neural network approach for the steam gasification of palm oil waste using bottom ash and CaO. Renewable Energy 2019;132:243–54.
[23] Xing J, Wang H, Luo K, Wang S, Bai Y, Fan J. Predictive single-step kinetic model of biomass devolatilization for CFD applications: A comparison study of empirical correlations (EC), artificial neural networks (ANN) and random forest (RF). Renewable Energy 2019;136:104–14.
[24] Wang Y, Kinoshita C. Kinetic model of biomass gasification. Sol Energy 1993;51:19–25.
[25] Yu J, Smith JD. Validation and application of a kinetic model for biomass gasification simulation and optimization in updraft gasifiers. Chemical Engineering and Processing-Process Intensification 2018;125:214–26.
[26] Smith JD, Alembath A, Al-Rubaye H, Yu J, Gao X, Golpour H. Validation and application of a kinetic model for downdraft biomass gasification simulation. Chem Eng Technol 2019;42:2505–19.
[27] Yao Z, You S, Ge T, Wang C-H. Biomass gasification for syngas and biochar co-production: Energy application and economic evaluation. Appl Energy 2018;209:43–55.
[28] Yao Z, He X, Hu Q, Cheng W, Yang H, Wang C-H. A hybrid peripheral fragmentation and shrinking-core model for fixed-bed biomass gasification. Chem Eng J 2020;400:124940.
[29] Sommariva S, Grana R, Maffei T, Pierucci S, Ranzi E. A kinetic approach to the mathematical model of fixed bed gasifiers. Comput Chem Eng 2011;35:928–35.
[30] Babu B, Chaurasia A. Heat transfer and kinetics in the pyrolysis of shrinking biomass particle. Chem Eng Sci 2004;59:1999–2012.
[31] Wei L, Lu Y, Wei J. Hydrogen production by supercritical water gasification of biomass: Particle and residence time distribution in fluidized bed reactor. Int J Hydrogen Energy 2013;38:13117–24.
[32] Gerber S, Behrendt F, Oevermann M. An Eulerian modeling approach of wood gasification in a bubbling fluidized bed reactor using char as bed material. Fuel 2010;89:2903–17.
[33] Yoon H, Wei J, Denn MM. A model for moving-bed coal gasification reactors. AIChE J 1978;24:885–903.
[34] Hobbs M, Radulovic P, d.L. Smoot.. Combustion and gasification of coals in fixed-beds. Prog Energy Combust Sci 1993;19:505–86.
[35] Arthur J. Reactions between carbon and oxygen. Trans Faraday Soc 1951;47:164–78.
[36] Jones W, Lindstedt R. Global reaction schemes for hydrocarbon combustion. Combust Flame 1988;73:233–49.
[37] Varma AK, Chatwani AU, Bracco FV. Studies of premixed laminar hydrogen □ air flames using elementary and global kinetics models. Combust Flame 1986;64:233–6.
[38] Abbas MN. Modeling of porosity equation for water flow through packed bed of monosize spherical packing. Journal of engineering and development 2011;15:205–26.
[39] Ascher S, Watson I, You S. Machine learning methods for modelling the gasification and pyrolysis of biomass and waste. Renew Sustain Energy Rev 2021:111902.
[40] Couhert C, Salvador S, Commandre J-M. Impact of torrefaction on syngas production from wood. Fuel 2009;88:2286–90.
[41] Van der Meijden CM, Veringa HJ, Rabou LP. The production of synthetic natural gas (SNG): A comparison of three wood gasification systems for energy balance and overall efficiency. Biomass Bioenergy 2010;34:302–11.
[42] Huang F, Jin S. Investigation of biomass (pine wood) gasification: Experiments and Aspen Plus simulation. Energy Sci Eng 2019;7:1178–87.
[43] E. Fercher, H. Hofbauer, T. Fleck, R. Rauch, G. Veronik. **Two years experience with the FICFB-gasification process,** (1998).
[44] Sheth PN, Babu B. Production of hydrogen energy through biomass (waste wood) gasification. Int J Hydrogen Energy 2010;35:10803–10.
[45] Qin K, Lin W, Fæster S, Jensen PA, Wu H, Jensen AD. Characterization of residual particulates from biomass entrained flow gasification. Energy Fuels 2013;27:262–70.
[46] Plis P, Wilk R. Theoretical and experimental investigation of biomass gasification process in a fixed bed gasifier. Energy 2011;36:3838–45.
[47] Sheth PN, Babu B. Experimental studies on producer gas generation from wood waste in a downdraft biomass gasifier. Bioresour Technol 2009;100:3127–33.
[48] González WA, Pérez JF, Chapela S, Porteiro J. Numerical analysis of wood biomass packing factor in a fixed-bed gasification process. Renewable Energy 2018;121:579–89.
[49] Breiman L. **Random forests** Machine learning 2001;45:5–32.
[50] Wang Y, Liao Z, Mathieu S, Bin F, Tu X. Prediction and evaluation of plasma arc reforming of naphthalene using a hybrid machine learning model. J Hazard Mater 2021;404:123965.
[51] Yuan Y, Wu L, Zhang X. Gini-Impurity Index Analysis. IEEE Trans Inf Forensics Secur 2021;16:3154–69.
[52] Xing J, Luo K, Wang H, Gao Z, Fan J. A comprehensive study on estimating higher heating value of biomass from proximate and ultimate analysis with machine learning approaches. Energy 2019;188:116077.
[53] Dewi C, Chen R-C. Random forest and support vector machine on features selection for regression analysis. Int J Innov Comput Inf Control 2019;15:2027–37.
[54] Cutler DR, Edwards Jr TC, Beard KH, Cutler A, Hess KT, Gibson J, et al. Random forests for classification in ecology. Ecology 2007;88:2783–92.
[55] Ullah Z, Naqvi SR, Farooq W, Yang H, Wang S, Vo D-V-N. A comparative study of machine learning methods for bio-oil yield prediction–A genetic algorithm-based features selection. Bioresour Technol 2021;335:125292.
[56] García-Bacaicoa P, Mastral J, Ceamanos J, Berrueco C, Serrano S. Gasification of biomass/high density polyethylene mixtures in a downdraft gasifier. Bioresour Technol 2008;99:5485–91.
[57] Jayah T, Aye L, Fuller RJ, Stewart D. Computer simulation of a downdraft wood gasifier for tea drying. Biomass Bioenergy 2003;25:459–69.
[58] Zainal Z, Rifau A, Quadir G, Seetharamu K. Experimental investigation of a downdraft biomass gasifier. Biomass Bioenergy 2002;23:283–9.
[59] Simone M, Nicolella C, Tognotti L. Numerical and experimental investigation of downdraft gasification of woody residues. Bioresour Technol 2013;133:92–101.
[60] Lucas C, Szewczyk D, Blasiak W, Mochida S. High-temperature air and steam gasification of densified biofuels. Biomass Bioenergy 2004;27:563–75.
[61] Saw W, McKinnon H, Gilmour I, Pang S. Production of hydrogen-rich syngas from steam gasification of blend of biosolids and wood using a dual fluidised bed gasifier. Fuel 2012;93:473–8.
[62] Janajreh I, Al Shrah M. Numerical and experimental investigation of downdraft gasification of wood chips. Energy Convers Manage 2013;65:783–92.
[63] Aydin ES, Yucel O, Sadikoglu H. Experimental study on hydrogen-rich syngas production via gasification of pine cone particles and wood pellets in a fixed bed downdraft gasifier. Int J Hydrogen Energy 2019;44:17389–96.